

Article

# Selective Formation of Para-Xylene by Methanol Aromatization over Phosphorous Modified ZSM-5 Zeolites

Xianjun Niu <sup>1,2,\*</sup> , Kai Wang <sup>3,\*</sup>, Yang Bai <sup>1</sup>, Yi-en Du <sup>1</sup>, Yongqiang Chen <sup>1</sup>, Mei Dong <sup>2</sup> and Weibin Fan <sup>2</sup>

<sup>1</sup> College of Chemistry and Chemical Engineering, Jinzhong University, Jinzhong 030619, China; baiyang@jzxy.edu.cn (Y.B.); duye@jzxy.edu.cn (Y.-e.D.); chen Yongqiang82@126.com (Y.C.)

<sup>2</sup> State Key Laboratory of Coal Conversion, Institute of Coal Chemistry, Chinese Academy of Sciences, 27 South Taoyuan Road, Taiyuan 030001, China; mdong@sxicc.ac.cn (M.D.); fanwb@sxicc.ac.cn (W.F.)

<sup>3</sup> College of Chemical and Environmental Engineering, Anyang Institute of Technology, Anyang 455000, China

\* Correspondence: niuxj@jzxy.edu.cn (X.N.); wangkai1102@ayit.edu.cn (K.W.)

Received: 25 March 2020; Accepted: 28 April 2020; Published: 29 April 2020



**Abstract:** Phosphorous modified ZSM-5 zeolites were synthesized by incipient wetness impregnation. Their performances for the methanol to aromatics conversion (MTA) were subsequently evaluated and the relationship between the catalyst structure and performance was focused on. The obtained results indicated that the introduction of phosphorous resulted in the modification of the catalyst structure characteristics and acidic properties, i.e., the reduction in the external surface area and micropore volume, the narrowing of the pore size, and the decrease in the quantity and strength of acid sites. As a result, the P/HZSM-5 catalyst exhibited the enhanced selectivity for the para-xylene (PX) in xylene isomers and xylene in aromatics, and their increase degrees were intensified with the increasing P content. The selectivity of PX in X increased from 23.8% to nearly 90% when P content was 5 wt.%. Meanwhile, the selectivity of xylene in aromatics was enhanced from 41.3% to 60.2%.

**Keywords:** methanol to aromatics; para-xylene; selectivity; phosphorous modified ZSM-5

## 1. Introduction

Para-xylene (PX) is of great value since it is useful in manufacturing terephthalic acid, which is an intermediate in the manufacture of synthetic fibers. The catalytic process for producing PX has been paid much attention and become a quite competitive subject in the petrochemical industry [1,2]. The reactions of toluene disproportionation [3,4], transalkylation of benzene with trimethylbenzene [5,6] and toluene methylation [7–9] were used to produce PX. However, it is imperative to develop new technologies because of the depletion of oil. The conversion of methanol to hydrocarbons over acidic zeolite catalysts is now considered an important and feasible non-petroleum route to obtain valuable chemicals [10–18]. Therefore, it is a significant work to design a shape selectivity catalyst for high PX selectivity in methanol to aromatics conversion (MTA). The reaction of methanol to para-xylene (MTPX) is a new technology for the upgrading of coal, biomass or natural gas into liquid fuels, which makes the production process of PX less reliant on crude oil resource.

In recent decades, the selective production of PX via alkylation or disproportionation of toluene has been studied over various zeolites catalysts, such as ZSM-5, MCM-22, mordenite and Y zeolite [19–23]. Among these zeolite catalysts, ZSM-5 zeolite has attracted more attention because of the well-defined 10 membered-ring channels that are much more favorable to the diffusion of PX than that of OX (ortho-xylene) or MX (meta-xylene). Therefore, an excellent PX selectivity could be expected by modifying ZSM-5 zeolite appropriately. It is found that the para-selectivity and external surface acidity

are usually inversely related [10]. Meanwhile, zeolites are known as shape-selective catalysts due to the presence of micropores with a pore diameter close to the molecular diameter of the products. Hence, in order to obtain high PX selectivity, it is important to reduce the acid sites, decrease the external surface area or modify the pore-openings by post synthesis modification. A number of modification methods are reported to improve para-selectivity, including silanation [24,25], precooking [26] and metal/non-metal oxide impregnation [27,28]. Among them, the impregnation of phosphate species on ZSM-5 has been shown to be convenient and effective to achieve a high PX selectivity [3,29,30]. The earlier study by Kaeding and coworkers [27,31] showed that the oxides of phosphorus species in zeolite pores imparted a diffusion barrier in the micropores exhibiting an increase in the para selectivity. Védrine et al. [32] found that phosphorus species passivated acid sites primarily at the entrance of the channels of the zeolite and the strong acid sites remained unmodified. They concluded that the high selectivity for para isomers of xylene (X) were assumed to be related to the narrowing of the pore size and the zeolite framework phosphorus species, rather than to the modification of acid sites' strength. Janardhan and coworkers [30] reported that the introduction of phosphorous into ZSM-5 zeolite generated new acid sites with pore narrowing, which were formed by the interaction of phosphates with bridging hydroxyl groups of ZSM-5 zeolites in the micropores. The active sites generated monolayer islands over zeolite surface and narrowed the pore opening, leading to a high selectivity of PX for alkylation and disproportionation reactions. Recently, the non-petroleum route to produce PX through MTA reaction has been increasingly investigated. Miyake et al. [33] reported a Zn/ZSM-5@silicalite-1 core-shell zeolite catalyst which showed a high xylene yield and PX selectivity, and the yield of PX could reach 40.7%. Wei et al. [34] designed a Zn-P-Si-ZSM-5 catalyst which showed increased selectivity PX (89.6%) in X for MTA reaction. The catalyst was impregnated with a Zn and P over the ZSM-5 sample, and then SiO<sub>2</sub> was loaded by chemical liquid phase deposition (CLD) modification. Zhu et al. [2] prepared Mg-Zn-Si-HZSM-5 catalyst by using the CLD method with polyphenylmethylsiloxane and then introducing Zn and Mg through vacuum impregnation. The prepared catalyst showed a high selectivity of PX in X (98.9%) and a relatively long lifetime for the MTA.

In this work, the highly shape-selective P/HZSM-5 catalysts for the MTA reaction were prepared by incipient wetness impregnation with H<sub>3</sub>PO<sub>4</sub> as a source of phosphorus and the different amounts of loaded phosphorus were obtained by changing the concentration of H<sub>3</sub>PO<sub>4</sub> solution. Then, the obtained samples were investigated by X-ray powder diffraction (XRD), infrared spectra for pyridine adsorption (Py-IR), N<sub>2</sub> adsorption-desorption, temperature programmed desorption of NH<sub>3</sub> (NH<sub>3</sub>-TPD), solid-state magic angle spinning nuclear magnetic resonance (MAS NMR) and thermogravimetric analysis (TG). Due to the fine modification of pore size and acidic properties, the selectivity of PX in X and the selectivity for xylene in aromatics over P/HZSM-5 catalyst both increased.

## 2. Results and Discussion

### 2.1. Catalyst Characterization

As shown in Figure 1, all the zeolite catalysts exhibited the similar peaks, which were the typical MFI structure. (JCPDS no. 73-1138) No new diffraction peak could be observed after the introduction of P species, even at the loadings of 5 wt.% P. The results indicated that the introduction of P did not destroy the structure of ZSM-5 framework severely and P was highly dispersed in ZSM-5 zeolite. Also, the relative crystallinities of prepared catalysts as shown in Table 1 decreased evidently. The crystallinity of the ZSM-5 zeolite was reduced to 76.4% after the loading of 5 wt.% P, which was most likely due to the framework defects caused by a certain degree of dealumination of the framework [2], as illustrated in the following <sup>27</sup>Al MAS NMR results (Figure 6A). The surface area and pore volume of HZSM-5 and P/HZSM-5 samples calculated by nitrogen adsorption-desorption were shown in Table 1. The BET surface area, external surface area and micropore volume all obviously decreased with the increase in P doping concentration, while the mesopore volume was almost constant, which could be ascribed to the fact that the loadings of P species blocked or destroyed some micropores in HZSM-5

during the process of phosphorus modification [35]. This indicated that the phosphorus species were not only doped on the external surface but also in the ZSM-5 channels. Compared with the total surface area, the external surface area decreased more obviously. The external surface area had decreased by more than 57% with 5 wt.% P loading.

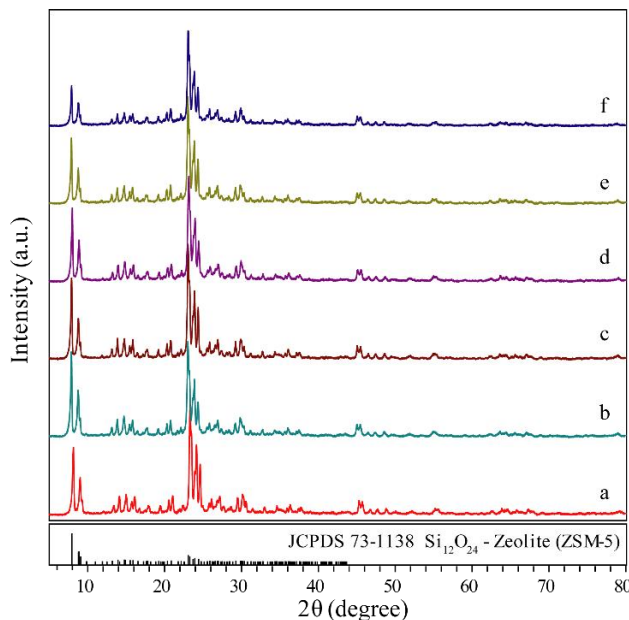


**Figure 1.** XRD patterns of the different catalysts: (a) HZSM-5, (b) 0.5% P/HZSM-5, (c) 1% P/HZSM-5, (d) 2% P/HZSM-5, (e) 3% P/HZSM-5 and (f) 5% P/HZSM-5.

**Table 1.** Textural properties of parent and P-modified HZSM-5 samples.

Samples	Crystallinity (%)	$S_{\text{BET}}$ ( $\text{m}^2\cdot\text{g}$ )	$S_e$ ( $\text{m}^2\cdot\text{g}$ )	$V_{\text{mes}}$ ( $\text{cm}^3\cdot\text{g}$ )	$V_{\text{mic}}$ ( $\text{cm}^3\cdot\text{g}$ )
HZSM-5	100	381	13.5	0.03	0.18
0.5% P/HZSM-5	96.2	360	12.9	0.04	0.17
1% P/HZSM-5	94.4	333	11.8	0.03	0.15
2% P/HZSM-5	87.6	311	9.4	0.03	0.14
3% P/HZSM-5	85.2	285	8.5	0.03	0.13
5% P/HZSM-5	76.4	246	5.8	0.04	0.10

Note:  $S_{\text{BET}}$ , BET surface area;  $S_e$ , external surface area, calculated by the t-plot method;  $V_{\text{mes}}$ , mesopore volume;  $V_{\text{mic}}$ , micropore volume, obtained by the t-plot method; the relative crystallinity is compared with the parent HZSM-5 having the strongest diffraction intensity.

The incorporation of phosphorus obviously influenced the porous structure of HZSM-5, as illustrated in Figure 2. The loading of P made the pore size distribution of HZSM-5 a little narrow and the pore size become remarkably smaller. The shrinkage of pore size in P modified HZSM-5 zeolites may be attributed to the formation of hydroxy-bridged P species in ZSM-5 zeolites or the accumulation of P species in the channels of ZSM-5 zeolites, which may impart a diffusion barrier and influence product diffusion in the micropores resulting in an increase in shape selectivity [30]. In order to reveal the probable relationship between the pore size and the catalytic properties, the adsorption isotherms of PX and MX on HZSM-5 and 5% P/HZSM-5 are shown in Figure 3. The adsorption results verified that m-xylene was more diffusion-limited than p-xylene on P modified HZSM-5 catalyst. This indicated that the introduction of P was beneficial to enhance the competitive adsorption of p-xylene because of pore narrowing. A similar phenomenon was found when  $\text{SiO}_2$  was loaded on the surface of the ZSM-5 catalyst. Compared with the unmodified ZSM-5 catalyst, the Si-modified catalyst enhanced the diffusion barrier in the mouth or channel of the zeolite and significantly inhibited the adsorption and diffusion of m-xylene [6].

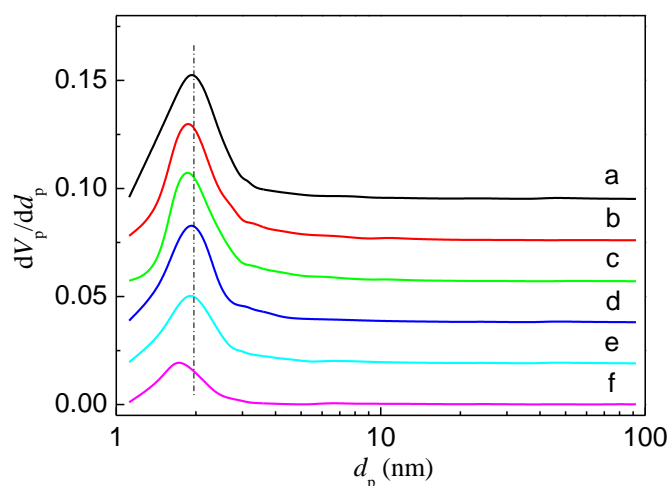


**Figure 2.** Pore size distribution of parent and P modified HZSM-5 zeolites: (a) HZSM-5, (b) 0.5% P/HZSM-5, (c) 1% P/HZSM-5, (d) 2% P/HZSM-5, (e) 3% P/HZSM-5 and (f) 5% P/HZSM-5.

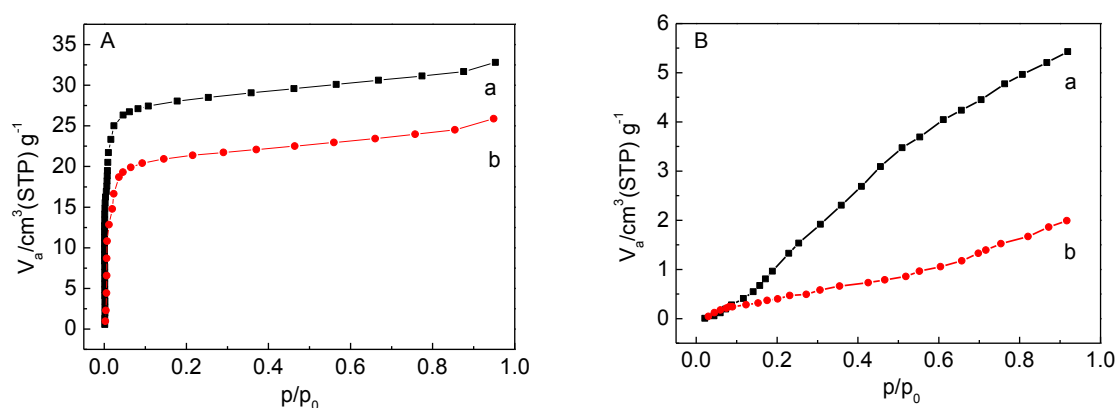


**Figure 3.** Adsorption isotherms of para-xylene (PX) (A) and meta-xylene (MX) (B) on HZSM-5 (a) and 5% P/HZSM-5 (b).

The total acid quantity and strength of acid sites in parent and P-modified HZSM-5 zeolites were obtained by  $\text{NH}_3$ -TPD, as shown in Figure 4. The HZSM-5 zeolite exhibited a typical  $\text{NH}_3$ -TPD profile with two characteristic peaks at about 190 and 380 °C, representing the ammonia adsorbed on the weak acid sites and strong acid sites, respectively [36]. After the doping with P, the evident changes in the peak temperature and area of the strong acid sites were observed. The peak temperature of the strong acid sites shifted towards a low temperature and the peak area decreased obviously. The more P doping was used, the smaller the peak area became, indicating that the decrease in the amount and strength of strong acid sites was due to the doping with P. The low-temperature peak also slightly shifted toward a low temperature, demonstrating that the loading of P also reduced weak acid strength. The difference was that the density of weak acid sites in low temperature was less affected with the increase in P loadings (as listed in Table 2).

Chemisorption of pyridine on HZSM-5 and P-modified HZSM-5 zeolites also illustrated the changes in zeolite acidity. As shown in Figure 5, all catalysts showed absorption peaks at about 1545 and 1450  $\text{cm}^{-1}$ , which were ascribed to pyridine chemisorbed on Brönsted (B) acid sites and pyridine adsorbed on Lewis (L) acid sites, respectively [37,38]. The incorporation of phosphorus led to a dramatic decline in the amount of both Brönsted and Lewis acidic sites. When small amounts of P were added ( $\leq 1$  wt.%), the acid amount of the Brönsted acid sites showed a sharp decrease compared to that of the Lewis acid sites (as listed in Table 2). Whereas, further increasing phosphorus content from 1 to 5 wt.% resulted in an evident decrease in the acid amount of the Lewis acid sites and a slight

decrease in the amount of the Brönsted acid sites. In summary, the loading of phosphorus reduced both the acid strength and amount of HZSM-5 zeolite, especially strong acid sites.

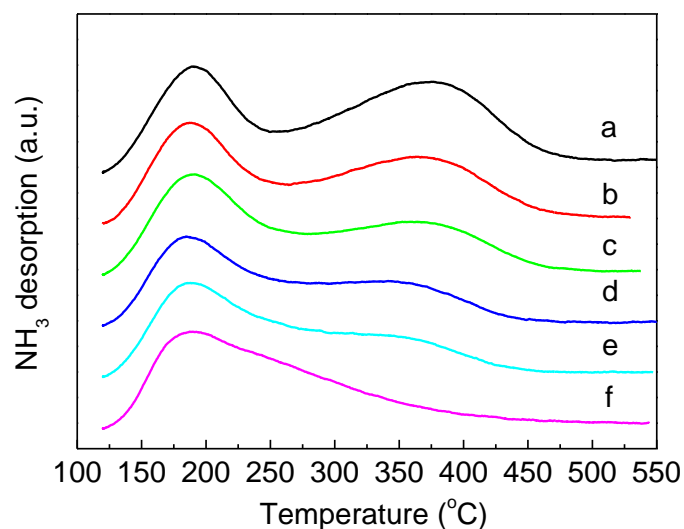


**Figure 4.** NH<sub>3</sub>-TPD profiles of parent and P-modified HZSM-5 zeolites: (a) HZSM-5, (b) 0.5% P/HZSM-5, (c) 1% P/HZSM-5, (d) 2% P/HZSM-5, (e) 3% P/HZSM-5 and (f) 5% P/HZSM-5.

**Table 2.** Acidity characterization of HZSM-5 and P/HZSM-5 zeolites.

Samples	Acidity by Strength <sup>a</sup> (mmol·g)			Acidity by Type <sup>b</sup> (mmol·g)		
	Strong	Weak	Total	Brönsted	Lewis	L/B
HZSM-5	0.32	0.20	0.52	0.170	0.054	0.32
0.5% P/HZSM-5	0.24	0.17	0.41	0.082	0.046	0.56
1% P/HZSM-5	0.18	0.19	0.37	0.079	0.033	0.42
2% P/HZSM-5	0.15	0.18	0.33	0.075	0.020	0.27
3% P/HZSM-5	0.13	0.20	0.33	0.073	0.009	0.12
5% P/HZSM-5	0.05	0.26	0.31	0.072	0.005	0.07

<sup>a</sup> Determined by NH<sub>3</sub>-TPD. <sup>b</sup> Obtained by Py-IR. L/B, the ratio of the amount of Lewis acidic sites to that of Brönsted acidic sites.

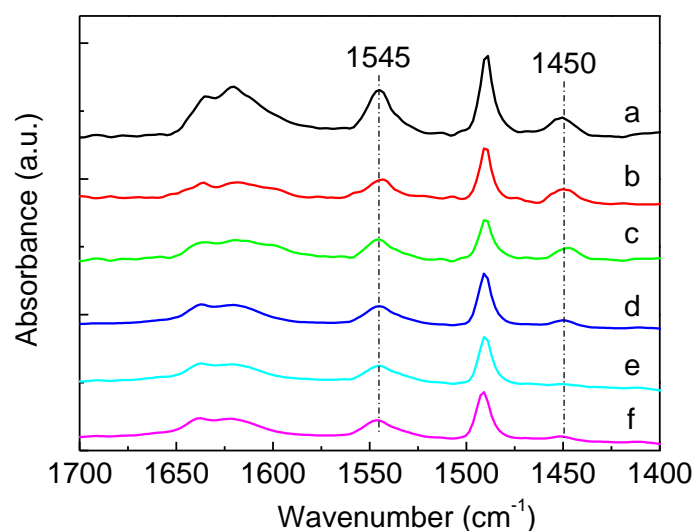


**Figure 5.** FT-IR spectra of pyridine adsorption on parent and P-modified HZSM-5 zeolites: (a) HZSM-5, (b) 0.5% P/HZSM-5, (c) 1% P/HZSM-5, (d) 2% P/HZSM-5, (e) 3% P/HZSM-5 and (f) 5% P/HZSM-5.

$^{27}\text{Al}$  MAS NMR has been extensively used as an effective technique to identify states of the Al atoms in the zeolite. Figure 6A showed  $^{27}\text{Al}$  MAS NMR spectra of HZSM-5 and P/HZSM-5 samples. For the parent HZSM-5 zeolite, a characteristic peak of typical Al species around 53 ppm was detected that could be ascribed to a tetrahedral framework aluminum [32]. A relatively weak signal appeared at 0 ppm which could be assigned to octahedral aluminum species, revealing that there existed a small number of extra-framework aluminum species in the HZSM-5 zeolite. With increasing impregnation degree, new peaks at about  $-14$  and  $40$  ppm appeared. The signal at  $-14$  ppm was related to octahedral aluminum interacting with a P atom [39]. The peak around  $40$  ppm was generally assigned to a tetrahedral framework aluminum or extra-framework aluminum species in a distorted environment [40]. With the increase in P loadings, the intensity of signals at  $-14$  and  $40$  ppm increased while that at  $53$  ppm decreased, illustrating that the dealumination of the HZSM-5 zeolite framework occurred as a result of the phosphate impregnation, consistent with the XRD, micropore volume and acidity measurement results.

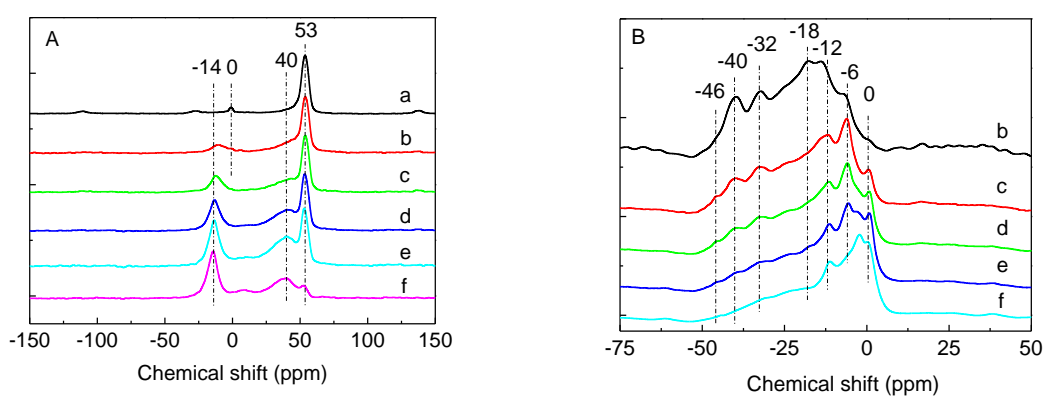


**Figure 6.**  $^{27}\text{Al}$  MAS NMR spectra (A) and  $^{31}\text{P}$  MAS NMR spectra (B) of parent and P-modified HZSM-5 zeolites: (a) HZSM-5, (b) 0.5% P/HZSM-5, (c) 1% P/HZSM-5, (d) 2% P/HZSM-5, (e) 3% P/HZSM-5 and (f) 5% P/HZSM-5.

The  $^{31}\text{P}$  MAS NMR spectra of P/HZSM-5 zeolites were shown in Figure 6B. The peak at 0 ppm was ascribed to excess P species which did not interact with framework aluminum. The signal around  $-6$  ppm was assigned to P species in pyrophosphoric acid or pyrophosphates, whereas the  $-12$  ppm signal was assigned to P species for intermediate groups in short-chain polyphosphates or pyrophosphates. The signals from  $-18$  to  $-40$  ppm were mainly due to extra-framework aluminophosphate and highly condensed polyphosphate complexes. Another signal appearing at  $-46$  ppm could be assigned to intermediate  $\text{P}_4\text{O}_{10}$  groups [32,41]. As can be seen in Figure 6B, the signals at 0 and  $-12$  ppm increased slightly with the increase in P content, whereas the peaks from  $-18$  to  $-40$  ppm decreased evidently. This indicated that the phosphorus content had a remarkable effect on the existent state of the phosphorus species, which may have an influence on the catalytic performance.

## 2.2. Influence of Phosphorus on the Catalytic Performance

The effect of phosphorus on the catalytic performance was illustrated in Figure 7 and Table 3. The introduction of phosphorus exhibited a significant impact on the catalytic stability, methanol conversion, and product selectivity. Compared with the unmodified HZSM-5, a small amount of phosphorus ( $\leq 1$  wt.%) could enhance the catalyst stability at a certain degree. Further increasing the P content, the catalyst stability and methanol conversion both decreased evidently. Equilibrium mixtures of xylene isomers generally contain only 23%–24% PX. As can be seen in Figure 7B, the PX selectivity in xylene was 23.8% on unmodified HZSM-5 zeolite. The introduction of phosphorus to HZSM-5 zeolite appreciably increased the selectivity for PX in xylene in the MTA reaction. The selectivity of PX in xylene increased with the increase in P content and it reached nearly to 90% when P content was

5 wt.%. Meanwhile, the selectivity for xylene in aromatics was enhanced with increasing the P content. The further detailed results were listed in Table 3. The modified catalysts also greatly improved the selectivity of light olefins ( $C_2^= \sim C_5^=$ ) and decreased the generation of aromatics and alkanes ( $C_1^- \sim C_4^-$ ).

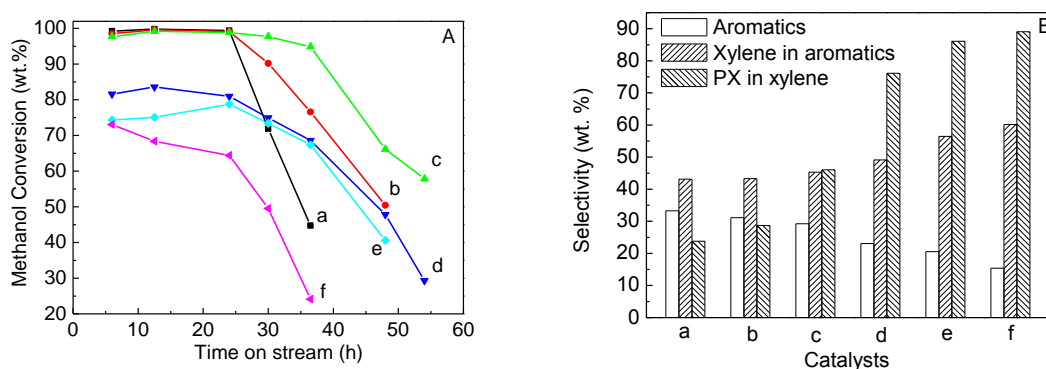


**Figure 7.** Methanol conversion with the time on stream (TOS) (A) and product selectivity at a TOS of 12.5 h (B) over parent and P-modified HZSM-5 zeolites: (a) HZSM-5, (b) 0.5% P/HZSM-5, (c) 1% P/HZSM-5, (d) 2% P/HZSM-5, (e) 3% P/HZSM-5 and (f) 5% P/HZSM-5.

**Table 3.** Products distribution of the methanol to aromatics (MTA) reaction over different catalysts.

Catalysts	Conv. <sub>MeOH</sub>	Production Selectivity (wt.%)					Xylene in Aromatics	PX in X	Yield of PX <sup>b</sup>
		$C_1^- \sim C_4^-$	$C_2^= \sim C_5^=$	$C_{5+}$ non-Aromatics	Aromatics	Others <sup>a</sup>			
HZSM-5	99.8	37.91	7.96	18.78	33.26	2.09	43.14	23.83	3.41
0.5% P/HZSM-5	99.6	34.20	8.29	24.43	31.14	1.94	43.30	28.70	3.86
1% P/HZSM-5	99.2	26.24	14.70	29.64	29.22	0.20	45.33	46.02	6.05
2% P/HZSM-5	83.6	16.59	42.74	16.33	23.05	1.29	49.12	76.14	7.21
3% P/HZSM-5	75.1	11.96	49.75	16.65	20.57	1.07	56.44	86.12	7.51
5% P/HZSM-5	68.4	10.73	62.42	9.86	15.42	1.57	60.16	89.05	5.65

<sup>a</sup> Others,  $H_2$  and  $CO_X$ ; <sup>b</sup> the yield of PX is calculated through methanol conversion  $\times$  aromatics selectivity  $\times$  xylene selectivity in aromatics  $\times$  PX selectivity in X; Conv.<sub>MeOH</sub>, methanol conversion. The data were obtained at 12.5 h.

Generally, in the MTA reaction, methanol is dehydrated to form dimethyl ether with the action of protons, which can be converted to light olefins by further dehydration and methylation. The light olefins are further developed into  $C_{5+}$  non-aromatic hydrocarbons by polymerization and cyclization. Then the aromatics and alkanes are generated by hydrogen transfer and dehydro-cyclization reactions under the action of Brønsted acid sites [14,42]. The results of acidity measurement showed that the amount of the Brønsted acid sites decreased obviously after the doping of P, which was consistent with the changes in the selectivity of aromatics and alkanes. In addition, because phosphorus can enter the channels of catalyst and cover the strong acid sites of the inner surface, the amount and strength of strong acid sites decreased significantly with P doping, resulting in the poor methanol conversion [43].

The spent catalysts were studied using thermogravimetric analysis. The weight loss of the samples on the range of 300–750 °C revealed the decomposition of coke deposition [9]. As shown in Figure 8, the amounts of coke deposition in the used P/HZSM-5 catalysts decreased to a certain extent. Especially, increasing P content to more than 1% resulted in an obvious decrease in coke amounts. As can be seen from the catalytic performance (Figure 7 and Table 3), when P content was above 1%, the catalyst stability and methanol conversion both decreased evidently, whereas the selectivity of PX in X improved greatly. The phenomenon may be due to the fact that high level loadings of P blocked more pore volume and external surface area, which reduced the resistance of coke deposition of the catalyst. The narrowed pore size led by the introduction of P limited the diffusion of products and made the micropore entrance block quickly, resulting in a fast coke deposition rate and deactivation of the catalyst.

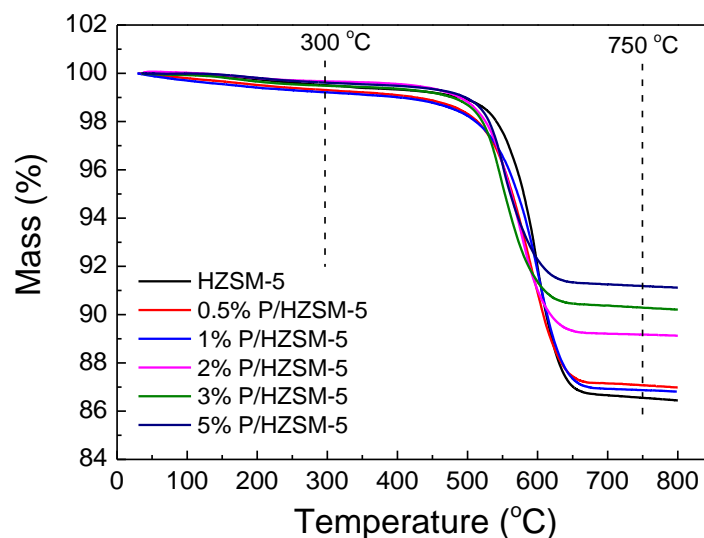


**Figure 8.** Thermogravimetric analysis (TG) curves of the spent HZSM-5 and P/HZSM-5 catalysts.

Meanwhile, the introduction of P reduced external surface area and narrowed the pore size, leading to an increase in the selectivity of xylene and PX. It is reported that the narrowing of the pore openings and the poisoning of external acid sites can enhance the PX selectivity in X isomers in MTA reaction [2]. Firstly, the narrowed pore size made the generation of PX easier than that of other X isomers and C<sub>9+</sub> aromatics, and the small amount of other X isomers and C<sub>9+</sub> aromatics formed was also difficult to diffuse out the zeolite channel. Moreover, the isomerization reaction of PX was inhibited after PX diffusing to the external surface which was poisoned by P species [42]. Therefore, the P/HZSM-5 was highly shape-selective for PX in the MTA reaction. However, the PX yield did not increase significantly as expected because of the decrease in the selectivity of aromatics and methanol conversion. The previous work found that the introduction of Zn species could generate the Zn-Lewis acid sites, which was beneficial to the formation of aromatics through the dehydration and cyclization reactions of light olefins [14]. Therefore, it is suggested that the catalyst with a high aromatics selectivity and high PX selectivity could be obtained by loading Zn over 5% P/HZSM-5.

### 3. Materials and Methods

#### 3.1. Catalyst Preparation

To obtain the sample with uniform crystal size, ZSM-5 zeolite was synthesized by seed-induction synthesis. The silicalite-1 seed was synthesized by modifying the procedures reported in reference [44]. The obtained colloidal silicalite-1 was directly used as a seed to prepare ZSM-5 zeolites. ZSM-5 samples were synthesized with the molar composition: SiO<sub>2</sub>:0.011Al<sub>2</sub>O<sub>3</sub>:0.02Na<sub>2</sub>O:0.15TPAOH:30H<sub>2</sub>O prepared from silica sol (30 wt.% SiO<sub>2</sub>), sodium aluminate (NaAlO<sub>2</sub>, Al<sub>2</sub>O<sub>3</sub> ≥ 41 wt.%), tetrapropylammonium hydroxide (TPAOH, 48.67 wt.% in aqueous solution). The synthesis mixture was conducted at 170 °C in a teflon-lined, stainless-steel autoclave under rotation (20 r/min). The obtained samples were recovered by centrifugation and repeatedly re-suspended in distilled water to remove physically attached templates. The recovered samples were dried at 100 °C overnight and calcined at 560 °C for 10 h in air, repeatedly ion-exchanging Na<sup>+</sup> with aqueous NH<sub>4</sub>NO<sub>3</sub> solution (1 M, m(liquid)/m(solid) = 40) at 80 °C for 6 h, and subsequently calcined at 560 °C for 6 h.

Incipient wetness impregnation was used to incorporate Phosphorous species into HZSM-5 and the different phosphorous content was obtained by changing the concentration of H<sub>3</sub>PO<sub>4</sub> solution, then dried at 100 °C overnight and calcined at 560 °C for 6 h under ambient condition.

### 3.2. Catalyst Characterization

X-ray powder diffraction (XRD) patterns were collected on a Rigaku MiniFlex II desktop X-ray diffractometer (Rigaku, Tokyo, Japan) with monochromated Cu  $K\alpha$  radiation (30 kV and 15 mA). By assuming that the zeolite sample had the largest peak area in the range of  $2\theta$  from  $22^\circ$  to  $25^\circ$  (here, it was the parent HZSM-5), as a reference had a crystallinity of 100%, the relative crystallinity of the P/HZSM-5 catalyst was then estimated by comparing its total peak area in this  $2\theta$  range with that of the parent HZSM-5.

Nitrogen adsorption/desorption isotherms were measured at  $-196^\circ\text{C}$  on a BELSORP-max gas adsorption analyzer (MicrotracBEL, Osaka, Japan). The adsorption isotherms of p-xylene and m-xylene on the zeolites were measured at  $25^\circ\text{C}$  on the BELSORP-max instrument. The measurement process and result analysis were similar to those described in our previous work [14]. Similarly, temperature-programmed desorption of  $\text{NH}_3$  (AutoChem II 2920 chemisorption analyzer, Micromeritics, Atlanta, GA, USA) ( $\text{NH}_3$ -TPD, to obtain the amount and strength of acid sites), and infrared spectra for pyridine adsorption (Tensor 27 FT-IR spectrometer, Bruker, Karlsruhe, Germany) (Py-IR, to get the acidity of Brønsted and Lewis acidic sites [45]), were performed by following similar procedures with the same apparatus as reported previously [12,14].

Solid-state NMR investigations were performed on Bruker Avance III 600 spectrometer (Bruker, Karlsruhe, Germany).  $^{31}\text{P}$  MAS NMR was recorded with 85% phosphoric acid as the reference at 161.9 MHz with a pulse length of 3  $\mu\text{s}$  ( $60^\circ$ ) and pulse interval of 60 s.  $^{27}\text{Al}$  MAS NMR was carried out with 1.0 M aqueous solution of  $\text{Al}(\text{NO}_3)_3$  as the reference at 104.3 MHz, with the pulse of 1.7  $\mu\text{s}$ , and a pulse interval of 60 s. All the data were acquired at a spinning speed of 8 kHz.

Coke deposition after MTA reactions was performed by TG on a Rigaku Thermo plus Evo TG 8120 instrument (Rigaku, Tokyo, Japan). The spent catalysts were combusted from room temperature to  $800^\circ\text{C}$  with a heating rate of  $10^\circ\text{C min}^{-1}$  in air.

### 3.3. Catalyst Evaluation

The MTA reaction was performed in a fixed-bed micro reactor (Pengxiang, Tianjin, China). The reaction was carried out with methanol WHSV of  $3.2\text{ h}^{-1}$  at  $390^\circ\text{C}$  and 0.5 MPa. The zeolite catalysts were crushed and sieved to 20–40 mesh and pretreated at reaction temperature for 8 h in a nitrogen flow. The gas and liquid products were separated with a cold trap and analyzed by gas chromatographs (7890A, Agilent, Palo alto, CA, USA). The specific parameters of GC were the same values as described previously [14].

## 4. Conclusions

The phosphorous-modified HZSM-5 zeolites were prepared by incipient wetness impregnation. The effect of phosphorous on the structure of HZSM-5 and its relationship with the catalytic performance of P/H-ZSM-5 catalysts in MTA was studied. The results indicated that the introduction of P could reduce micropore volume and external surface area, narrow the pore size and decrease the amount and strength of strong acid sites. The pore size and acid properties of zeolite were finely modified by introducing phosphorous, which resulted in the P/HZSM-5 catalyst enhancing the PX selectivity in X isomers for MTA reaction. The PX selectivity in X and the selectivity for xylene in aromatics both improved significantly with the increase in P content. However, excessive P ( $>1\%$ ) also resulted in the decrease in aromatic selectivity and methanol conversion. The PX selectivity (in xylene) could reach nearly to 90% when P content was 5 wt.%, while the selectivity of xylene in aromatics was enhanced from 41.3% to 60.2%. Owing to the decrease in the selectivity of aromatics and methanol conversion, the yield of PX needs to be further improved. It is suggested that the catalyst with a high PX selectivity in X and high PX yield could be obtained by loading Zn over 5% P/HZSM-5 which can generate the Zn-Lewis acid sites to enhance the formation of aromatics through the dehydration and cyclization reactions of light olefins.

**Author Contributions:** Conceptualization, X.N., M.D. and W.F.; Data curation, K.W. and Y.-e.D.; Formal analysis, X.N. and K.W.; Funding acquisition, X.N., Y.-e.D. and Y.C.; Investigation, Y.B.; Methodology, X.N.; Writing—original draft, X.N.; Writing—review and editing, X.N., K.W. and Y.C.. All authors have read and agreed to the published version of the manuscript.

**Funding:** This research received no external funding.

**Acknowledgments:** This work was financially supported by the Doctor Research Funds of Jinzhong University, Scientific and Technological Innovation Programs of Higher Education Institutions in Shanxi (No. 2019L0881), the Applied Basic Research Project of Shanxi (No. 201901D111303), Shanxi “1331 Project” Key Innovative Research Team (PY201817), Jinzhong University “1331 Project” Key Innovative Research Team (jzxcyctd2017004 and jzxcyctd2019005) and the Research Project of Science and Technology of the Henan Province (202102310565).

**Conflicts of Interest:** The authors declare no conflict of interest.

## References

1. Pan, D.; Song, X.; Yang, X.; Gao, L.; Wei, R.; Zhang, J.; Xiao, G. Efficient and selective conversion of methanol to para-xylene over stable H[Zn,Al]ZSM-5/SiO<sub>2</sub> composite catalyst. *Appl. Catal. A* **2018**, *557*, 15–24. [[CrossRef](#)]
2. Li, J.; Tong, K.; Xi, Z.; Yuan, Y.; Hu, Z.; Zhu, Z. High-efficient conversion of methanol to p-xylene over shape-selective Mg-Zn-Si-HZSM-5 catalyst with fine modification of pore-opening and acidic properties. *Catal. Sci. Technol.* **2016**, *6*, 4802–4813. [[CrossRef](#)]
3. Kaeding, W.W.; Chu, C.; Young, L.B.; Butter, S.A. Shape-selective reactions with zeolite catalysts: II. Selective disproportionation of toluene to produce benzene and p-Xylene. *J. Catal.* **1981**, *69*, 392–398. [[CrossRef](#)]
4. Ji, Y.-J.; Zhang, B.; Xu, L.; Wu, H.; Peng, H.; Chen, L.; Liu, Y.; Wu, P. Core/shell-structured Al-MWW@B-MWW zeolites for shape-selective toluene disproportionation to para-xylene. *J. Catal.* **2011**, *283*, 168–177. [[CrossRef](#)]
5. Li, Y.; Wang, H.; Dong, M.; Li, J.; Wang, G.; Qin, Z.; Fan, W.; Wang, J. Optimization of Reaction Conditions in the Transalkylation of Toluene with 1,2,4-Trimethylbenzene Catalyzed by Beta Zeolite and the Investigation of Its Reaction Mechanism. *Acta Chim. Sin.* **2016**, *74*, 529–537. [[CrossRef](#)]
6. Cheng, X.; Wang, X.; Long, H. Transalkylation of benzene with 1,2,4-trimethylbenzene over nanosized ZSM-5. *Microporous Mesoporous Mater.* **2009**, *119*, 171–175. [[CrossRef](#)]
7. Lu, P.; Fei, Z.; Li, L.; Feng, X.; Ji, W.; Ding, W.; Chen, Y.; Yang, W.; Xie, Z. Effects of controlled SiO<sub>2</sub> deposition and phosphorus and nickel doping on surface acidity and diffusivity of medium and small sized HZSM-5 for para-selective alkylation of toluene by methanol. *Appl. Catal. A* **2013**, *453*, 302–309. [[CrossRef](#)]
8. Wang, C.; Zhang, Q.; Zhu, Y.; Zhang, D.; Chen, J.; Chiang, F.-K. p-Xylene selectivity enhancement in methanol toluene alkylation by separation of catalysis function and shape-selective function. *Mol. Catal.* **2017**, *433*, 242–249. [[CrossRef](#)]
9. Wang, C.; Wang, Y.; Chen, H.; Wang, X.; Li, H.; Sun, C.; Sun, L.; Fan, C.; Zhang, X. Effect of phosphorus on the performance of IM-5 for the alkylation of toluene with methanol into p-xylene. *C. R. Chim.* **2019**, *22*, 13–21. [[CrossRef](#)]
10. Pannida, D.; Chularat, W. A Comprehensive Review of the Applications of Hierarchical Zeolite Nanosheets and Nanoparticle Assemblies in Light Olefin Production. *Catalysts* **2020**, *10*, 245.
11. Bjørgen, M.; Akyalcin, S.; Olsbye, U.; Benard, S.; Kolboe, S.; Svelle, S. Methanol to hydrocarbons over large cavity zeolites: Toward a unified description of catalyst deactivation and the reaction mechanism. *J. Catal.* **2010**, *275*, 170–180. [[CrossRef](#)]
12. Niu, X.; Gao, J.; Wang, K.; Miao, Q.; Dong, M.; Wang, G.; Fan, W.; Qin, Z.; Wang, J. Influence of crystal size on the catalytic performance of H-ZSM-5 and Zn/H-ZSM-5 in the conversion of methanol to aromatics. *Fuel Process. Technol.* **2017**, *157*, 99–107. [[CrossRef](#)]
13. Wang, K.; Dong, M.; Niu, X.; Li, J.; Qin, Z.; Fan, W.; Wang, J. Highly active and stable Zn/ZSM-5 zeolite catalyst for the conversion of methanol to aromatics: effect of support morphology. *Catal. Sci. Technol.* **2018**, *8*, 5646–5656.
14. Niu, X.; Gao, J.; Miao, Q.; Dong, M.; Wang, G.; Fan, W.; Qin, Z.; Wang, J. Influence of preparation method on the performance of Zn-containing HZSM-5 catalysts in methanol-to-aromatics. *Microporous Mesoporous Mater.* **2014**, *197*, 252–261. [[CrossRef](#)]
15. Chang, N.; Bai, L.; Zhang, Y.; Zeng, G. Fast synthesis of hierarchical CHA/AEI intergrowth zeolite with ammonium salts as mineralizing agent and its application for MTO process. *Chem. Pap.* **2019**, *73*, 221–237. [[CrossRef](#)]

16. Li, N.; Meng, C.; Liu, D. Deactivation kinetics with activity coefficient of the methanol to aromatics process over modified ZSM-5. *Fuel* **2018**, *233*, 283–290. [[CrossRef](#)]
17. Jin, W.; Ma, J.; Ma, H.; Li, X.; Wang, Y. Hydrothermal synthesis of core-shell ZSM-5/SAPO-34 composite zeolites and catalytic performance in methanol-to-aromatics reaction. *J. Catal.* **2015**, *330*, 558–568. [[CrossRef](#)]
18. Li, H.; Dong, P.; Ji, D.; Zhao, X.; Li, C.; Cheng, C.; Li, G. Effect of the Post-Treatment of HZSM-5 on Catalytic Performance for Methanol to Aromatics. *ChemistrySelect* **2020**, *5*, 3413–3419. [[CrossRef](#)]
19. Van Vu, D.; Miyamoto, M.; Nishiyama, N.; Ichikawa, S.; Egashira, Y.; Ueyama, K. Catalytic activities and structures of silicalite-1/H-ZSM-5 zeolite composites. *Microporous Mesoporous Mater.* **2008**, *115*, 106–112.
20. Wu, P.; Komatsu, T.; Yashima, T. Selective formation of p-xylene with disproportionation of toluene over MCM-22 catalysts. *Microporous Mesoporous Mater.* **1998**, *22*, 343–356. [[CrossRef](#)]
21. Tsai, T.-C.; Liu, S.-B.; Wang, I. Disproportionation and transalkylation of alkylbenzenes over zeolite catalysts. *Appl. Catal. A* **1999**, *181*, 355–398. [[CrossRef](#)]
22. Van der Mynsbrugge, J.; Visur, M.; Olsbye, U.; Beato, P.; Bjørgen, M.; Van Speybroeck, V.; Svelle, S. Methylation of benzene by methanol: Single-site kinetics over H-ZSM-5 and H-beta zeolite catalysts. *J. Catal.* **2012**, *292*, 201–212. [[CrossRef](#)]
23. Dumitriu, E.; Hulea, V.; Kaliaguine, S.; Huang, M.M. Transalkylation of the alkylaromatic hydrocarbons in the presence of ultrastable Y zeolites Transalkylation of toluene with trimethylbenzenes. *Appl. Catal. A* **1996**, *135*, 57–81. [[CrossRef](#)]
24. Zhu, Z.; Xie, Z.; Chen, Q.; Kong, D.; Li, W.; Yang, W.; Li, C. Chemical liquid deposition with polysiloxane of ZSM-5 and its effect on acidity and catalytic properties. *Microporous Mesoporous Mater.* **2007**, *101*, 169–175. [[CrossRef](#)]
25. Zheng, S.; Heydenrych, H.R.; Jentys, A.; Lercher, J.A. Influence of Surface Modification on the Acid Site Distribution of HZSM-5. *J. Phys. Chem. B* **2002**, *106*, 9552–9558. [[CrossRef](#)]
26. Bauer, F.; Chen, W.H.; Bilz, E.; Freyer, A.; Sauerland, V.; Liu, S.B. Surface modification of nano-sized HZSM-5 and HFER by pre-coking and silanization. *J. Catal.* **2007**, *251*, 258–270. [[CrossRef](#)]
27. Chen, N.Y.; Kaeding, W.W.; Dwyer, F.G. Para-directed aromatic reactions over shape-selective molecular sieve zeolite catalysts. *J. Am. Chem. Soc.* **1979**, *101*, 6783–6784. [[CrossRef](#)]
28. Li, Y.; Xie, W.; Yong, S. The Acidity and Catalytic Behavior of Mg ZSM 5 Prepared via Solid State Reaction. *Appl. Catal. A* **1997**, *150*, 231–242. [[CrossRef](#)]
29. Kaeding, W.W.; Chu, C.; Young, L.B.; Weinstein, B.; Butter, S.A. Selective alkylation of toluene with methanol to produce para-Xylene. *J. Catal.* **1981**, *67*, 159–174. [[CrossRef](#)]
30. Janardhan, H.L.; Shanbhag, G.V.; Halgeri, A.B. Shape-selective catalysis by phosphate modified ZSM-5: Generation of new acid sites with pore narrowing. *Appl. Catal. A* **2014**, *471*, 12–18. [[CrossRef](#)]
31. Kaeding, W.W.; Young, L.B.; Chu, C.-C. Shape-selective reactions with zeolite catalysts: IV. Alkylation of toluene with ethylene to produce p-ethyltoluene. *J. Catal.* **1984**, *89*, 267–273. [[CrossRef](#)]
32. Védrine, J.C.; Auroux, A.; Dejaifve, P.; Ducarme, V.; Hoser, H.; Zhou, S. Catalytic and physical properties of phosphorus-modified ZSM-5 zeolite. *J. Catal.* **1982**, *73*, 147–160. [[CrossRef](#)]
33. Miyake, K.; Hirota, Y.; Ono, K.; Uchida, Y.; Tanaka, S.; Nishiyama, N. Direct and selective conversion of methanol to para-xylene over Zn ion doped ZSM-5/silicalite-1 core-shell zeolite catalyst. *J. Catal.* **2016**, *342*, 63–66. [[CrossRef](#)]
34. Zhang, J.; Qian, W.; Kong, C.; Wei, F. Increasing para-Xylene Selectivity in Making Aromatics from Methanol with a Surface-Modified Zn/P/ZSM-5 Catalyst. *ACS Catal.* **2015**, *5*, 2982–2988. [[CrossRef](#)]
35. Blasco, T.; Corma, A.; Martínez-Triguero, J. Hydrothermal stabilization of ZSM-5 catalytic-cracking additives by phosphorus addition. *J. Catal.* **2006**, *237*, 267–277. [[CrossRef](#)]
36. Zhang, L.; Zhang, H.; Chen, Z.; Liu, S.; Ren, J. Effect of framework Al siting on catalytic performance in methanol to aromatics over ZSM-5 zeolites. *J. Fuel Chem. Technol.* **2019**, *47*, 1468–1475. [[CrossRef](#)]
37. Zhao, G.; Teng, J.; Xie, Z.; Jin, W.; Yang, W.; Chen, Q.; Tang, Y. Effect of phosphorus on HZSM-5 catalyst for C 4-olefin cracking reactions to produce propylene. *J. Catal.* **2007**, *248*, 29–37. [[CrossRef](#)]
38. Palella, A.; Barbera, K.; Arena, F.; Spadaro, L. Clean Syn-Fuels via Hydrogenation Processes: Acidity–Activity Relationship in O-Xylene Hydrotreating. *ChemEngineering* **2020**, *4*, 4. [[CrossRef](#)]
39. Caeiro, G.; Magnoux, P.; Lopes, J.M.; Ribeiro, F.R.; Menezes, S.M.C.; Costa, A.F.; Cerqueira, H.S. Stabilization effect of phosphorus on steamed H-MFI zeolites. *Appl. Catal. A* **2006**, *314*, 160–171. [[CrossRef](#)]

40. Li, P.; Zhang, W.; Han, X.; Bao, X. Conversion of Methanol to Hydrocarbons over Phosphorus-modified ZSM-5/ZSM-11 Intergrowth Zeolites. *Catal. Lett.* **2010**, *134*, 124–130. [[CrossRef](#)]
41. Dyballa, M.; Klemm, E.; Weitkamp, J.; Hunger, M. Effect of Phosphate Modification on the Brønsted Acidity and Methanol-to-Olefin Conversion Activity of Zeolite ZSM-5. *Chem. Ing. Tech.* **2013**, *85*, 1719–1725. [[CrossRef](#)]
42. Zhu, X.; Zhang, J.; Cheng, M.; Wang, G.; Yu, M.; Li, C. Methanol Aromatization over Mg-P-Modified [Zn,Al]ZSM-5 Zeolites for Efficient Coproduction of para-Xylene and Light Olefins. *Ind. Eng. Chem. Res.* **2019**, *58*, 19446–19455. [[CrossRef](#)]
43. Ghiaci, M.; Abbaspur, A.; Arshadi, M.; Aghabarari, B. Internal versus external surface active sites in ZSM-5 zeolite: Part 2: Toluene alkylation with methanol and 2-propanol catalyzed by modified and unmodified H<sub>3</sub>PO<sub>4</sub>/ZSM-5. *Appl. Catal. A* **2007**, *316*, 32–46. [[CrossRef](#)]
44. Li, Q.H.; Mihailova, B.; Creaser, D.; Sterte, J. The nucleation period for crystallization of colloidal TPA-silicalite-1 with varying silica source. *Microporous Mesoporous Mater.* **2000**, *40*, 53–62. [[CrossRef](#)]
45. Ferreira Madeira, F.; Ben Tayeb, K.; Pinard, L.; Vezin, H.; Maury, S.; Cadran, N. Ethanol transformation into hydrocarbons on ZSM-5 zeolites: Influence of Si/Al ratio on catalytic performances and deactivation rate. Study of the radical species role. *Appl. Catal. A* **2012**, *443–444*, 171–180. [[CrossRef](#)]



© 2020 by the authors. Licensee MDPI, Basel, Switzerland. This article is an open access article distributed under the terms and conditions of the Creative Commons Attribution (CC BY) license (<http://creativecommons.org/licenses/by/4.0/>).